Received 16 September 2025; revised 19 December 2025; accepted 15 January 2026. Date of publication 20 January 2026; date of current version 13 February 2026. The review of this article was arranged by Associate Editor M. Geronazzo.

Digital Object Identifier 10.1109/OJSP.2026.3656057

Design of Acoustic Equalization Filters for Headphones Based on Low-Rank Regularization

FLORIAN HILGEMANN AND PETER JAX (Member, IEEE)

Institute of Communication Systems, RWTH Aachen University, 52062 Aachen, Germany

CORRESPONDING AUTHOR: FLORIAN HILGEMANN (e-mail: hilgemann@iks.rwth-aachen.de).

Open access funding provided by the Open Access Publishing Fund of RWTH Aachen University.

ABSTRACT The use of equalization filters to achieve acoustic transparency can improve the sound quality of hearables and hearing aids. Finite impulse response (FIR) filters guarantee stability and offer a listening impression close to the open ear, but their implementation may conflict with the resource constraints typical of hearing devices. Infinite impulse response (IIR) filters are commonly used to meet these constraints, but their design often lacks stability and performance guarantees. Therefore, we consider indirect IIR filter design methods that extend FIR filter designs with an IIR approximation step. To mitigate the performance degradation caused by the IIR approximation, we establish a formal connection between optimization variable and IIR approximation error, and propose an approximation-aware design algorithm based on the nuclear norm heuristic. The evaluation considers the design of hear-through filters using real-world measurement data. The proposed approach can reduce the time-domain mean-squared error by up to 6 dB compared to conventional methods, and shows a high robustness against between-person variance. Thus, the results offer an improvement in hearing device personalization within practical constraints.

INDEX TERMS Acoustic transparency, headphones, hearables, infinite impulse response filter, personalization.

I. INTRODUCTION

Hearing devices such as hearables have gained tremendous popularity in recent years. The convergence of hearables and hearing aids led to over-the-counter (OTC) hearing aids, which facilitate to consume media content, engage in far-end communication, and provide auditory aid [1], [2], [3]. However, wearing such devices alters the auditory impression compared to the open ear. Wearers will recognize this as a muffled perception of ambient sounds with restricted spatial hearing capabilities [4], [5], [6].

These effects can be mitigated using digital signal processing algorithms. More specifically, a natural perception of ambient sounds while wearing hearables can be achieved to a great extent by using a hear-through filter [7], [8], [9], [10], [11], [12]. These filters utilize an outward-facing microphone with loudspeaker playback to augment sounds that reach the listener's eardrum. OTC hearing aid users may fine-tune the equalization to their preferences, e.g., based on an estimated hearing loss [13]. To emphasize the conceptual similarity to classical equalizers, this is referred to as "equalization".

The equalization is sensitive towards variations in the electro-acoustic transfer paths. These paths are wearer- and situation-dependent and thus unknown a priori, but can be estimated, e.g., by a user-initiated calibration algorithm [14], [15], [16]. Similar to the akin head-related transfer function (HRTF) personalization problem [17], [18], [19], this bears the potential to improve the listening impression.

To implement acoustic equalization, adaptive [20], [21], [22] or fixed filters [10], [11] can be used, and the focus of this work is on the latter. Due to their guaranteed performance and stability, FIR filters that minimize a time- or frequency-domain minimum mean square error (MMSE) criterion are widely adopted. In addition, generalizations of the MMSE approach that aim for improved spatial hearing capabilities [23], [24], [25], or robustness against variations in the acoustic transfer paths [26] were investigated.

Although digital signal processors (DSPs) are becoming increasingly capable, the algorithmic complexity remains crucial in practice because most hearables are battery-powered. The implied resource constraints add an interesting yet challenging issue to the matter that is studied in more detail in this work. A low-complexity approach close at hand is to use FIR filters with few taps. This has shown promising results in some applications, e.g., open-fitting hearing aids [10]. However, FIR filters do not constitute a general low-order solution because the transfer paths might imply the need to use long impulse responses that are not computationally feasible.

Compared to FIR filters, IIR filters can implement long impulse responses at a fraction of the complexity [27]. However, the design often relies on non-convex optimization and requires constraints to guarantee stability of the filter [28], [29], [30]. These methods are well-suited for "offline" designs which determine the filter coefficients beforehand, but their lack of guarantees contradicts the requirements of a personalization at runtime.

Indirect methods to IIR filter design serve as another approach that consists of two stages: first, a high-order prototype FIR filter is designed using one of the previously mentioned approaches, followed by an IIR approximation step [31], [32], [33]. However, although stability can be guaranteed, the IIR approximation error made in the second step can severely degrade the equalization performance, which can lead to unreliable results.

To overcome these obstacles, we proposed an indirect acoustic equalization filter design method that yields low-order IIR filters with guaranteed stability in our previous work [34], [35]. The method is based on the well-researched nuclear norm heuristic, which has found application, e.g., in model reduction, system identification, or image restoration problems [36], [37], [38], [39], [40]. Applied to acoustic equalization filters, Hankel nuclear norm regularization (HNNR) penalizes the IIR approximation error using convex optimization methods, which ultimately improves the performance.

This paper extends our previous work [34] by considering two aspects that are critical for practical applications. First, it has been shown for other applications that the nuclear norm introduces a bias that may reduce the performance [41], [42], [43], [44]. We show empirically that this also applies in the considered application, and employ an iterative bias compensation method [41] to improve the performance. Such methods were proposed for image processing applications, and are not directly applicable to digital filter design problems. To enable their application, the present work establishes a novel connection between filter coefficient vector and IIR approximation error. Second, we conduct extensive application-oriented simulations that highlight the effect of the algorithm parameters. They provide insights into the mechanism of the algorithms and recommendations for practical applications.

The paper is structured as follows: Section II introduces the notation and problem statement while Section III revisits conventional indirect IIR filter design methods. In Section IV, the proposed filter optimization based on HNNR and a bias-compensated extension are described. Application examples are presented in Section V, and Section VI concludes the paper.

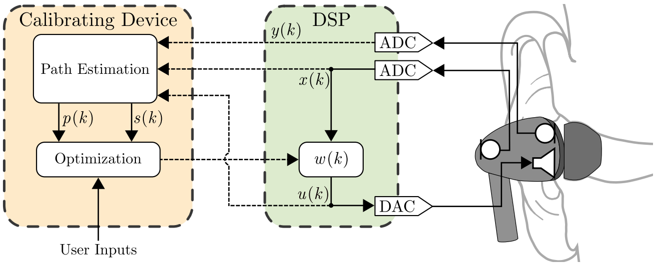

FIGURE 1. System components of in-ear headphones and corresponding model variables.

II. ACOUSTIC EQUALIZATION IN HEADPHONES

Fig. 1 shows the schematic layout of the considered hearing device. It features outward- and inward-facing microphones, a loudspeaker, and a DSP that the equalization algorithm is implemented on. Its goal is to augment listener-perceived sounds to improve the listening impression. Since DSPs are often resource-constrained, the filter optimization is outsourced to a separate, more capable calibrating device [45]. This could be a phone or laptop that communicates with the DSP, which allows to consider the interaction of wearer and device in the optimization.

This work utilizes a digital linear time-invariant (LTI) model with sampling time t_s and corresponding sampling rate $f_\mathrm{s} = 1/t_\mathrm{s}$. The discrete-time index is denoted k with $t = kt_\mathrm{s}$, and t denoting the time in seconds. For simplicity, the model excludes electrical noise and quantization noise, as well as non-linear distortions. Lowercase letters indicate time-domain signals, whereas uppercase letters denote their frequency-domain representation (e.g., $X(z)$ is the z-transform of $x(k)$). In contrast, lowercase and uppercase letters in bold type denote column vectors and matrices, respectively.

When the sound playback is switched off, i.e., for $u(k) = 0$, the ear canal signal is given by $y(k) = x(k) * p(k)$. Here, $p(k)$ refers to the impulse response of the primary path $P(z)$, which is defined as the relative transfer function from the outward-facing microphone to an inward-facing microphone, thereby reflecting the passive insulation, and "$*$" denotes discrete-time convolution. Sound playback is modeled using the discrete-time secondary path $S(z)$, which reflects the characteristics of the inward-facing microphone, loudspeaker, and converters.

A. PROBLEM STATEMENT

The algorithm aims to improve the listening impression by pre-filtering the ambient signal with the feed-forward filter impulse response $w(k)$ as $u(k) = x(k) * w(k)$. The signal $u(k)$ is played back over the secondary path, which yields the inner microphone signal

$$y(k) = x(k) * \left[p(k) + s(k) * w(k)\right]. \tag{1}$$

The sub-expression $h(k) = p(k) + s(k) * w(k)$ in (1) is often referred to as the impulse response of the aided transfer path

$$H(z) = \frac{Y(z)}{X(z)} = P(z) + S(z)W(z), \tag{2}$$

which results from the z-transform of (1) for $X(z) \neq 0$.

The problem considered in this work is to optimize the feed-forward filter $W(z)$ so that the aided transfer path $H(z)$ resembles a target path $D(z)$ as close as possible. This general formulation facilitates the implementation of several modes of operation, e.g., $D(z) = 0$ aims to suppress ambient sounds as in active noise cancelling (ANC) headphones, whereas a shifted unit impulse $D(z) = z^{-k_0}$ with a modeling delay of k_0 samples acts against the passive insulation of headphones to provide acoustic transparency of ambient sounds [10], [11].

In theory, any design target $D(z)$ can be attained without error using the optimal feed-forward filter

$$W^{(\mathrm{o})}(z) = \frac{D(z) - P(z)}{S(z)}. \tag{3}$$

Unfortunately, (3) is not practically feasible: $W^{(\mathrm{o})}(z)$ is generally acausal or unstable since $S(z)$ is not always minimum phase. Moreover, the order of $W^{(\mathrm{o})}(z)$ is determined by the orders of $P(z)$, $S(z)$ and $D(z)$, which might exceed the DSP's computational capacity. Instead, the goal pursued in this work is to provide optimal equalization performance in practical applications with calibration information and resource constraints: for given paths $P(z)$ and $S(z)$, find a stable N-th order IIR feed-forward filter $W(z)$ which yields an aided path $H(z)$ that reflects $D(z)$ as closely as possible.

III. CONVENTIONAL INDIRECT IIR FILTER DESIGN

The indirect method is widely used to design IIR filters based on two steps. First, a high-order prototype FIR filter is designed so that the performance requirements are met. Second, this prototype filter is approximated by an N-th order IIR filter. In many applications the order will be fixed, e.g., to values in the order of 5 to 20, depending on the DSP.

A. PROTOTYPE FIR FILTER DESIGN

The optimization of FIR filters for acoustic equalization is well studied. For a clear presentation, the MMSE filter design based on a time-domain formulation [11], [26], [46] is revisited. In this case, $w(k)$ is an FIR filter with L_w filter coefficients that are determined as outlined below.

We introduce the auxiliary convolution sequences

$$a(k) = x(k) * s(k), \tag{4a}$$

$$b(k) = x(k) * \left[p(k) - d(k)\right] \tag{4b}$$

to write the deviation of the target impulse response from the aided impulse response, weighted by a given ambient signal $x(k)$, as

$$e(k) = x(k) * \left[p(k) + s(k) * w(k) - d(k)\right] \tag{5a}$$

$$= a(k) * w(k) + b(k). \tag{5b}$$

If we further approximate the paths $p(k)$ and $s(k)$ as length-L_p FIR filters and the outer signal $x(k)$ as a length-L_x sequence, then the error $e(k)$ only attains non-zero values for $0 \leq k < L_a + L_w - 1$, where $L_a = L_b = L_p + L_x - 1$ denotes the length of the convolution sequences $a(k)$ and $b(k)$.

Writing the unknown filter coefficients in vector form

$$\boldsymbol{w} = \begin{bmatrix} w(0) & w(1) & \cdots & w(L_w - 1) \end{bmatrix}^{\mathrm{T}} \tag{6}$$

allows to quantify the energy of the residual error $e(k)$ through an MMSE loss using compact matrix notation

$$f(\boldsymbol{w}) = \frac{1}{2} \|\boldsymbol{A}\boldsymbol{w} + \boldsymbol{b}\|_2^2. \tag{7}$$

Here, $\boldsymbol{A} \in \mathbb{R}^{(L_a+L_w-1)\times L_w}$ is a convolution matrix, i.e., a Toeplitz matrix with constant entries on the diagonal and the off-diagonals, and $\boldsymbol{b} \in \mathbb{R}^{L_a+L_w-1}$ is the residual vector. They are defined as

$$\boldsymbol{A} = \begin{bmatrix} a(0) & 0 & \dots & 0 \\ \vdots & \ddots & \ddots & \vdots \\ a(L_a-1) & \ddots & \ddots & 0 \\ 0 & \ddots & \ddots & a(0) \\ \vdots & \ddots & \ddots & \vdots \\ 0 & \dots & 0 & a(L_a-1) \end{bmatrix}, \boldsymbol{b} = \begin{bmatrix} b(0) \\ \vdots \\ b(L_a-1) \\ 0 \\ \vdots \\ 0 \end{bmatrix}. \tag{8}$$

The FIR filter coefficient vector that is optimal in the MMSE sense is uniquely determined by

$$\boldsymbol{w}^{(\mathrm{LS})} = \underset{\boldsymbol{w}}{\operatorname{argmin}}\, f(\boldsymbol{w}) = -\left(\boldsymbol{A}^{\mathrm{T}}\boldsymbol{A}\right)^{-1}\boldsymbol{A}^{\mathrm{T}}\boldsymbol{b}. \tag{9}$$

We refer to [11], [26], [46], [47] for variants of the MMSE approach with improved robustness against transfer path variations, frequency-dependent regularization, or acausality management. These approaches use different MMSE criteria that imply different $\boldsymbol{A}$ and $\boldsymbol{b}$ matrices, but are not investigated further here for the sake of brevity.

B. IIR FILTER APPROXIMATION

Step two of the indirect method is to approximate the given prototype filter $W(z)$ by an N-th order IIR filter $\widetilde{W}(z)$ with $N < L_w - 1$. In the following, a tilde is used to denote quantities that result from this IIR approximation. Prony's method [48], iterative least-squares methods [49], [50], [51], [52], or state space methods such as balanced truncation (BT) [53], [54], [55], [56] could be used, among others. Autoregressive methods such as the Yule-Walker method [57] are not considered as they do not aim to match the phase response of $W(z)$.

Of these methods, BT appears to be suitable in the context of this work: it yields estimates with a low error and guarantees filter stability [53]. A BT algorithm that is fine-tuned for FIR-by-IIR approximation was proposed in [55]. This algorithm utilizes the Hankel matrix

$$\mathcal{H}(\boldsymbol{w}) = \begin{bmatrix} w(1) & w(2) & \cdots & w(L_w-1) \\ w(2) & & ⋰ & 0 \\ \vdots & ⋰ & ⋰ & \vdots \\ w(L_w-1) & 0 & \cdots & 0 \end{bmatrix}, \tag{10}$$

where $\mathcal{H}(\boldsymbol{w})$ maps a length-L_w vector onto a square matrix of dimension $L_w - 1$. Note that $\mathcal{H}(\boldsymbol{w})$ does not contain the feedthrough coefficient $w(0)$, and that the script letter $\mathcal{H}$ is used to avoid confusion with the aided transfer path $H(z)$.

The singular value decomposition (SVD) $\mathcal{H}(\boldsymbol{w}) = \boldsymbol{U}\boldsymbol{\Sigma}\boldsymbol{V}^{\mathrm{T}}$ is computed, where $\boldsymbol{U}$ and $\boldsymbol{V}$ are unitary matrices, and $\boldsymbol{\Sigma} = \mathrm{diag}(\sigma_1, \ldots, \sigma_{L_w-1})$ is a diagonal matrix. The singular values are sorted by magnitude in descending order, i.e., $\sigma_i \geq \sigma_{i+1}\ \forall\, i \geq 1$, and are commonly referred to as Hankel singular values (HSVs). For a given order N, the BT algorithm divides $\mathcal{H}(\boldsymbol{w})$ into two subspaces

$$\mathcal{H}(\boldsymbol{w}) = \boldsymbol{U}\boldsymbol{\Sigma}\boldsymbol{V}^{\mathrm{T}} = \boldsymbol{U}_1\boldsymbol{\Sigma}_1\boldsymbol{V}_1^{\mathrm{T}} + \boldsymbol{U}_2\boldsymbol{\Sigma}_2\boldsymbol{V}_2^{\mathrm{T}}, \tag{11}$$

where $\boldsymbol{U}_1\boldsymbol{\Sigma}_1\boldsymbol{V}_1^{\mathrm{T}}$ is termed "strong subspace" with $\boldsymbol{\Sigma}_1 = \mathrm{diag}(\sigma_1, \ldots, \sigma_N)$ containing only the N largest HSVs. Essentially, BT discards the "weak subspace" $\boldsymbol{U}_2\boldsymbol{\Sigma}_2\boldsymbol{V}_2^{\mathrm{T}}$ by evaluating linear matrix expressions detailed in [55]. This yields an N-th order IIR filter $\widetilde{W}(z)$ in state space form, which can be converted to another preferred representation such as a direct form filter [56].

The intuition behind BT is that the strong subspace reveals the filter's most important components. The subdivision into strong and weak subspaces is uniquely determined by the HSVs, and ensures that $\boldsymbol{U}_1\boldsymbol{\Sigma}_1\boldsymbol{V}_1^{\mathrm{T}}$ explains most variance.

IV. PROPOSED APPROXIMATION-AWARE DESIGN

The prototype FIR filter $W(z)$ provides optimal performance, but this generally does not hold true for the IIR filter $\widetilde{W}(z)$ which results from indirect IIR filter design methods. Instead, the IIR approximation error can significantly degrade the equalization performance in resource-constrained applications. In this section, we show how indirect approaches can be augmented to reduce the IIR approximation error. From a methodological point of view, this corresponds to an extension of the methods [39], [41] to inverse filtering problems.

A. CONCEPT

Motivated by the limited control over the IIR approximation error that conventional indirect methods provide, we propose to combine both steps of the indirect filter design method. More specifically, we extend the prototype filter design to be aware of the post hoc IIR filter approximation. The proposal is based on the relationship between the Hankel matrix $\mathcal{H}(\boldsymbol{w})$ and the IIR approximation error.

If BT is used for the approximation, there exists an error bound [56]: at any frequency, the IIR filter $\widetilde{W}(z)$ deviates from the given prototype filter $W(z)$ by no more than twice the sum of the discarded HSVs, i.e.,

$$\|W(z) - \widetilde{W}(z)\|_\infty \leq 2 \sum_{i=N+1}^{L_w-1} \sigma_i = 2\,\mathrm{Tr}(\boldsymbol{\Sigma}_2). \tag{12}$$

Equation (12) implies a low IIR approximation error if $\mathcal{H}(\boldsymbol{w})$ has only few dominant HSVs when using BT. Because (12) provides a sound theoretical basis, we use BT for the IIR approximation in the following. Our goal is to extend the optimization of the prototype FIR filter $W(z)$ to promote sparsity in the singular value vector to reduce the contribution of $\mathrm{Tr}(\boldsymbol{\Sigma}_2)$ in (12).

To weigh the equalization performance against the IIR approximation error, the MMSE loss could be extended as

$$\underset{\boldsymbol{w}}{\operatorname{argmin}}\, f(\boldsymbol{w}) + \mu\,\mathrm{Tr}(\boldsymbol{\Sigma}_2) \tag{13}$$

with a scalar regularization parameter $\mu \geq 0$. This problem is inherently non-convex, except for the trivial case $L_w - 1 = N$, so it is tedious to solve in general [58]. As an alternative that is amenable to a personalization at runtime, we explore related approaches based on convex optimization in the following.

B. HANKEL NUCLEAR NORM REGULARIZATION (HNNR)

In order to promote low IIR approximation errors, we propose to adopt the well-researched nuclear norm heuristic to influence the singular value decay of $\mathcal{H}(\boldsymbol{w})$. The nuclear norm $\|\cdot\|_*$ of a matrix is defined as the sum over all singular values. For the Hankel matrix of interest, this corresponds to the sum of all HSVs:

$$\|\mathcal{H}(\boldsymbol{w})\|_* = \sum_{i=1}^{L_w-1} \sigma_i = \mathrm{Tr}(\boldsymbol{\Sigma}_1) + \mathrm{Tr}(\boldsymbol{\Sigma}_2). \tag{14}$$

As a regularizer, it aims to induce sparsity in the vector of HSVs and behaves similar to the ℓ_1 norm for vectors [59]. In the present application, we use the nuclear norm to reduce the IIR approximation error in step two of the indirect method. A convex relaxation to (13) based on the nuclear norm reads

$$\underset{\boldsymbol{w}}{\operatorname{argmin}}\, f(\boldsymbol{w}) + \mu\,\|\mathcal{H}(\boldsymbol{w})\|_*. \tag{15}$$

Its main advantage is that it falls into the category of convex problems, which simplifies the optimization. Problem (15) can be solved in polynomial time and with guaranteed global optimality using efficient numerical solvers [39], [60], [61], [62], [63].

A disadvantage of (15) is that the nuclear norm penalizes all HSVs although the IIR approximation error (12) only depends on the smallest HSVs. Problems (13) and (15) thus yield different results in general [36], [38]. The undesired penalization of the largest HSV can be mitigated by using a long prototype filter with $L_w \gg N$ and a careful selection of the regularization parameter μ.

C. BIAS-COMPENSATED HNNR

Although the previously described HNNR algorithm aims to reduce the IIR approximation error, it does not consider the divergent requirements on the smallest versus the largest HSVs that the error bound (12) implies. Instead, it penalizes all HSVs. This causes a bias of the HSVs towards zero that can lead to a performance degradation. This was observed for image processing problems, for which bias compensation methods have been developed [41], [42]. However, the algorithms presented therein are not directly applicable to digital filter design problems because the involved images assume that matrix entries can be chosen independently of each other. In contrast, the inverse filter design problem requires matrices with Hankel and Toeplitz structure to model convolutions and the IIR filter approximation in the optimization. We enable the application of these methods to filter design problems by establishing an explicit relationship between the filter coefficient vector and the bias based on (12).

Suppose the matrices $\boldsymbol{U}_1$ and $\boldsymbol{V}_1$ in (11) are known. Using the SVD's orthonormality properties $\boldsymbol{U}_1^{\mathrm{T}}\boldsymbol{U}_1 = \boldsymbol{V}_1^{\mathrm{T}}\boldsymbol{V}_1 = \boldsymbol{I}$ and $\boldsymbol{U}_1^{\mathrm{T}}\boldsymbol{U}_2 = \boldsymbol{V}_2^{\mathrm{T}}\boldsymbol{V}_1 = \boldsymbol{0}$, one identifies the strong subspace HSVs as $\boldsymbol{U}_1^{\mathrm{T}}\mathcal{H}(\boldsymbol{w})\boldsymbol{V}_1 = \boldsymbol{\Sigma}_1$. This yields the nuclear norm of the weak subspace

$$\|\mathcal{H}(\boldsymbol{w})\|_* - \mathrm{Tr}\left(\boldsymbol{U}_1^{\mathrm{T}}\mathcal{H}(\boldsymbol{w})\boldsymbol{V}_1\right) = \mathrm{Tr}(\boldsymbol{\Sigma}_2), \tag{16}$$

which corresponds to the error bound (12) with scaling by a factor 1/2. The main obstacle to using (16) in the optimization is that it is non-convex because $\boldsymbol{U}_1$ and $\boldsymbol{V}_1$ depend on $\boldsymbol{w}$. As an alternative, we propose an alternating optimization of convex problems similar to [41]. This involves repeatedly solving the bias-compensated problem

$$\underset{\boldsymbol{w}}{\mathrm{argmin}}\, f(\boldsymbol{w}) + \mu\left(\|\mathcal{H}(\boldsymbol{w})\|_* - \mathrm{Tr}\left(\widehat{\boldsymbol{U}}_1^{\mathrm{T}}\mathcal{H}(\boldsymbol{w})\widehat{\boldsymbol{V}}_1\right)\right) \tag{17}$$

with matrices $\widehat{\boldsymbol{U}}_1$ and $\widehat{\boldsymbol{V}}_1$, which remain fixed during optimization but are updated between optimizations. These matrices reflect estimates of the strong subspace basis matrices $\boldsymbol{U}_1$ and $\boldsymbol{V}_1$ to penalize only the weak subspace according to (13). An initial estimate of the strong subspace basis matrices is required. For this, the least-squares solution $\boldsymbol{w}^{(\mathrm{LS})}$ appears to be well-suited.

Problem (17) is convex because (15) is convex, and $\mathrm{Tr}(\widehat{\boldsymbol{U}}_1^{\mathrm{T}}\mathcal{H}(\boldsymbol{w})\widehat{\boldsymbol{V}}_1)$ is a linear function of $\boldsymbol{w}$. The main advantage of solving (17) as an approximation to (13) is that (17) admits the use of efficient solvers with convergence and optimality guarantees whereas (13) does not. The optimization can be conducted by estimating $\widehat{\boldsymbol{U}}_1$ and $\widehat{\boldsymbol{V}}_1$ iteratively as described by Algorithm 1:

This algorithm, termed BC-HNNR, integrates knowledge about the IIR approximation into the optimization. The key difference to [41] is that we employ the strong subspace basis matrices which the BT algorithm relies on. This incorporates the FIR-by-IIR filter approximation into the prototype filter optimization.

As the iteration converges, the estimates $\widehat{\boldsymbol{U}}_1$ and $\widehat{\boldsymbol{V}}_1$ will approach $\boldsymbol{U}_1$ and $\boldsymbol{V}_1$, respectively. It is possible that these

Algorithm 1: Bias-compensated HNNR (BC-HNNR).

1: **Input** $\boldsymbol{A}, \boldsymbol{b}, \mu, N, K$
2: $\boldsymbol{w}^{(0)} \leftarrow \boldsymbol{w}^{(\mathrm{LS})}$
3: **for** $k = 0, 1, \ldots, K-1$ **do**
4: construct $\mathcal{H}(\boldsymbol{w}^{(k)})$ using (10)
5: estimate $\widehat{\boldsymbol{U}}_1^{(k)}$ and $\widehat{\boldsymbol{V}}_1^{(k)}$ using (11)
6: update $\boldsymbol{w}^{(k+1)}$ by solving (17)
7: **end for**
8: **Output** $\boldsymbol{w}^{(K)}$

$\boldsymbol{U}_1$ and $\boldsymbol{V}_1$ matrices correspond to the global optimum of (13), however, this is not guaranteed due to the inherent non-convexity. Since the algorithm is based on convex subproblems, it is nevertheless possible to ensure a high degree of reliability. This is examined further in Section V.

The computational effort to solve problems (15) and (17) is roughly $\mathcal{O}(L_w^4)$ operations [61]. This is more costly compared to solving (9) at about $\mathcal{O}(L_w^3)$ operations. Nevertheless, the algorithm can be implemented in practice while taking into account the resource constraints of the DSP by outsourcing the optimization onto a separate device, as shown in Fig. 1.

V. EVALUATION

Both proposed algorithms are subjected to an application-oriented evaluation based on real-world measurement data. The personalization of a hear-through filter using in-ear headphones is considered. The performance and the robustness of the proposed HNNR and BC-HNNR algorithms against transfer path variations are investigated and compared to conventional algorithms with equal implementation complexity on the DSP. Insights into the effect of the IIR filter order and the regularization parameter are provided, and the bias compensation mechanism that BC-HNNR utilizes is examined. Based on these investigations, suggestions for a practical parameterization of the algorithms are derived.

A. EXPERIMENTAL SETUP

The study considers IIR filter optimization for acoustic transparency. A sampling rate $f_s = 24\,\mathrm{kHz}$ is used, and IIR filter orders between $N = 1$ and $N = 16$ are considered. The design target is set to a unit impulse $d(k) = \delta(k - k_0)$ with modeling delay $k_0 = 5$. This corresponds to a spectrally flat target magnitude response with a delay of about 0.2 ms that acts as an acausality management [26]. The delay is below the audible threshold of 5 ms reported in [64].

The goal is to accommodate user-dependent properties such as ear geometries and headphone fittings to personalize the IIR filter for specific wearers. Related variations of the acoustic transfer paths $P(z)$ and $S(z)$ are unknown a-priori, but the paths can be estimated at runtime [15], [16], [17], [18], [19]. To facilitate the reproducibility of the results, we use impulse responses $p(k)$ and $s(k)$ for different wearers and for two headphone designs from open-access databases [65], [66] which are briefly described below.

The PANDAR database [65] contains impulse responses for 23 wearers of Bose QuietComfort 20 in-ear headphones. They feature dynamic drivers and a closed housing as used in hearables and OTC hearing aids, and were modified to exclude the vendor's ANC electronics. The paths $P(z)$ and $S(z)$ are defined towards the device's inward-facing microphone.

In contrast, the hearpiece database [66] considers headphones with balanced armature receivers. These headphones are similar to traditional hearing aids and feature multiple microphones and loudspeakers. For comparability with the dynamic driver headphones, a single-channel hear-through implementation is considered. Here, $P(z)$ is defined as relative transfer function path from the outer vent to the eardrum microphone, and $S(z)$ is derived from the inner driver and the eardrum microphone responses for 24 wearers.

A limitation is that the optimization depends on $x(k)$, which is unknown a-priori. The communication between DSP and a separate calibrating device implies that knowledge on the statistics of $x(k)$ could be collected at runtime. We note that this offers further potential for improvement, but consider this aspect out of scope. As suggested in [46], we set $x(k) = \delta(k)$. This corresponds to a spectrally flat excitation, which can improve the robustness of the solution.

B. FILTER OPTIMIZATION

The proposed HNNR filter optimization was configured to use a prototype filter length $L_w = 512$ and the subsequent IIR filter approximation used the BT algorithm. To ensure an optimal configuration, the regularization parameter μ was chosen by solving (15) using the alternating directions method of multipliers (ADMM) with 32 candidate parameters μ_m sampled from a logarithmic grid with $10^{-6} \leq \mu_m \leq 10^1$ and $1 \leq m \leq 32$. This was performed individually for each wearer, and the IIR filter with minimal loss function value was selected for further considerations. This required to evaluate the impulse response of $\widetilde{W}(z)$, which is denoted as $\widetilde{\boldsymbol{w}}$. The proposed BC-HNNR variant used a different μ parameter obtained from solving (17) iteratively using Algorithm 1 with $L_w = 512$ and $K = 10$ iterations for the same candidate parameters μ_m. In our experiments, the optimization converged reliably in all cases, i.e., with both proposed algorithms, both devices, and all wearers.

We consider several established methods to compare the hear-through performance. The classical indirect filter design is a natural reference approach. It was implemented using the MMSE filter $\boldsymbol{w}^{(\mathrm{LS})}$ with $L_w = 512$. The approximation by an N-th order IIR filter was configured to use BT, which guarantees stability [55]. A more recently proposed indirect approach for use with headphones [33] is further considered. It utilizes an iterative least-squares IIR filter approximation proposed by Brandenstein and Unbehauen [51], [52] with a line-search mechanism. We set its iteration number to 10, and refer to the approach as "BU" in the following.

Direct IIR filter design methods are included in the evaluation as well. A simple approach which yields stable N-order filters is to design a short FIR filter with $L_w = N + 1$. Further, the least-squares fit to the optimal filter given by (3) using the damped Gauss-Newton algorithm [50] as implemented by the MATLAB function `invfreqz` is considered. It was configured to use a maximum of 10 iterations, which guarantees filter stability. For this method, equal numerator and denominator filter orders were chosen, and a 2^{18}-point Fourier transform was used. Lastly, the fixed-pole (FP) method [67], [68] is considered. This approach estimates fixed poles using the target filter and optimizes the zeros in a separate step. This method uses the Steiglitz-McBride iteration [49] as described in [67]. We initially used 10 iterations to determine the poles, but reduced the iteration number to 5 after encountering numerical problems. This resolved those issues and slightly improved the performance. Other direct methods such as [28], [29], [30] are not considered because they require manual tuning, e.g., because the stability is either not guaranteed or depends on the numerical solver used.

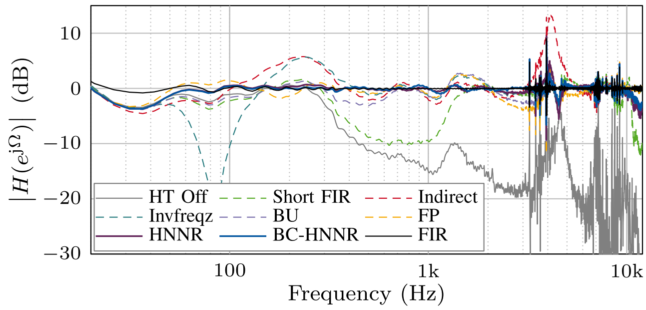

(a) Magnitude responses.

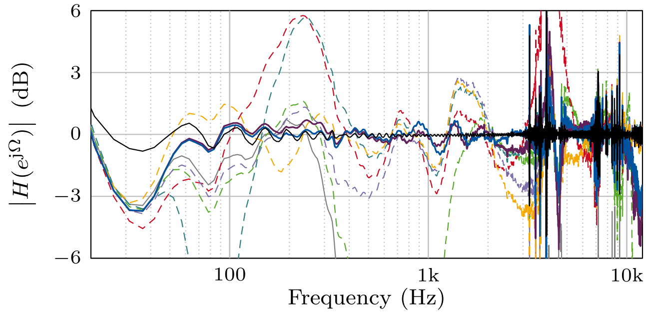

(b) Zoom into Fig. 2a.

FIGURE 2. Magnitude response of aided transfer path for one person wearing dynamic driver headphones. Dashed lines indicate conventional low-order filter design algorithms.

C. DYNAMIC DRIVER HEADPHONES HEAR-THROUGH

This section investigates the design and performance of a hear-through filter for the Bose QC20 in-ear headphones. Fig. 2 shows the magnitude of the aided transfer paths which are obtained from using the conventional and proposed algorithms for one specific wearer from the PANDAR database. The case "HT Off", which corresponds to inserted headphones with an inactive hear-through, is shown for reference. It highlights the effect of passive insulation, which mostly affects frequencies above 230 Hz. For better clarity, Fig. 2(b) shows the same results as Fig. 2(a), but with a scaled y-axis.

All hear-through systems aimed for a flat 0 dB response. The FIR filter achieved this with deviations of less than 1 dB at most frequencies, but using a much higher filter order. In contrast, the IIR filters use $N = 12$, which is amenable to an implementation on resource-constrained DSPs. Although all IIR filters counteracted the passive attenuation to a large extent, abrupt transitions which are inherent to the dataset [65] remained. The indirect method corresponds to using $\boldsymbol{w}^{(\mathrm{LS})}$ with subsequent IIR filter approximation. This caused unwanted peaks in the aided transfer path that degrade the performance, e.g., between 100 Hz and 300 Hz or at 4 kHz. These peaks were less pronounced with the other methods, but they produced undershoots at other frequencies. The proposed HNNR and BC-HNNR methods resulted in a smaller overall deviation from 0 dB than the other methods.

The loss function values $f(\widetilde{\boldsymbol{w}})$ which measure the mean-squared error for a given IIR filter are furthermore considered. Their values are proportional to the areas above and below the 0 dB line in Fig. 2, and they confirm the aforementioned observations: while the conventional indirect method achieves $f(\widetilde{\boldsymbol{w}}) = 0.334$ and the short FIR, invfreqz, BU and FP methods achieve 0.082, 0.025, 0.024, and 0.028, respectively, the proposed HNNR and BC-HNNR achieve 0.025 and 0.013, respectively. At equal system order, BC-HNNR yields roughly half of the time-domain impulse response error (i.e., a 6 dB reduction) compared with the best of the conventional methods.

Although invfreqz and HNNR yield roughly the same loss in this example, Fig. 2 shows that HNNR and BC-HNNR both result in a more even distribution of the error over frequency. Wearers are likely to perceive the two hear-through systems differently because notches and, especially, peaks of $|H(e^{\mathrm{j}\Omega})|$ have a major impact on the subjective listening impression [69]. The HNNR and BC-HNNR yield less pronounced peaks and notches compared to the indirect approach due to the IIR approximation error bound (12), which states that a reduction of $\mathrm{Tr}(\boldsymbol{\Sigma}_2)$ reduces the worst-case IIR approximation error over frequency.

One interesting observation is the difference in regularization parameters between HNNR and BC-HNNR. In this example, $\mu = 1.8 \cdot 10^{-4}$ lead to optimal results for HNNR, whereas a larger parameter $\mu = 1.2 \cdot 10^{-2}$ was favorable for BC-HNNR. This suggests that the bias compensation penalizes the IIR approximation error in a more targeted manner, which allows choosing greater μ values.

Fig. 3 details the loss function values $f(\boldsymbol{w})$ that the personalized filters achieve for all 23 wearers. The figure provides insight into the robustness against transfer path variations. The comparison is conducted with an equal filter order $N = 12$. Algorithms can be regarded as robust against these variations if both, the loss function value is low on average, and a low deviation between wearers is attained.

Although none of the algorithms reduced the loss below 10^{-1} for two of the wearers, they behave differently for the others. The median performance of the invfreqz method is in between the proposed HNNR and BC-HNNR methods, but it is less reliable because the loss is comparatively high for a few wearers. In contrast, the other conventional methods reduce these deviations slightly. The HNNR algorithm yields a similar robustness against transfer path variations, which the BC-HNNR improves upon by further reducing the best-case and worst-case loss.

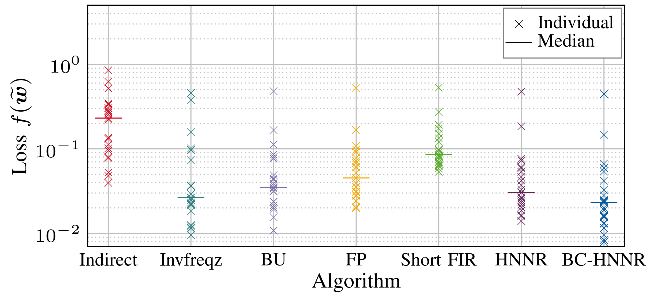

FIGURE 3. Loss function values for 23 wearers using dynamic driver headphones.

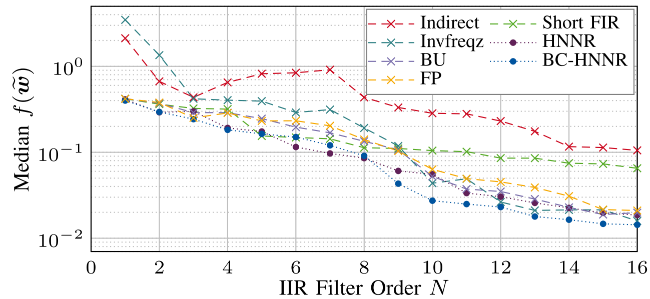

FIGURE 4. Median of loss function values with 23 wearers using dynamic driver headphones.

The experiment is repeated for different IIR filter orders $1 \leq N \leq 16$ in order to investigate the impact of N on the performance. Fig. 4 shows the median of the performances that the personalized filters achieved for all 23 wearers. The general trend is that the performance benefits from high filter orders, but the benefit manifests itself differently for the algorithms. At low orders, the indirect and invfreqz methods both yield large loss function values. However, the loss of the conventional indirect method stagnates for higher orders, whereas the loss of invfreqz improves by more than one order of magnitude. The performance of the BU approach was generally similar to FP, but tended to benefit more from using higher filter orders N.

In this experiment, the proposed BC-HNNR gave the lowest median loss for all considered orders except $N = 5$, where the short FIR filter was most promising, and $6 \leq N \leq 8$, where HNNR performed better. A possible explanation is the initial estimate of the strong subspace based on $\boldsymbol{w}^{(\mathrm{LS})}$, which can be unreliable at low filter orders. This is also reflected by the loss of the conventional indirect method, which turned out to be non-decreasing for $4 \leq N \leq 7$. The benefit of the

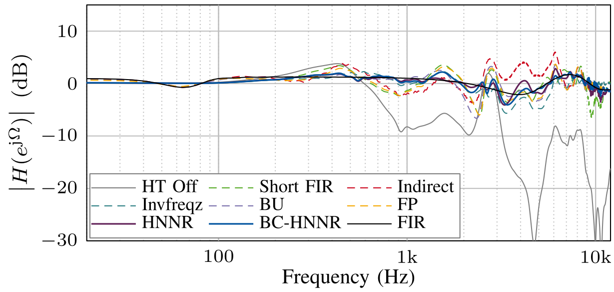

(a) Magnitude responses.

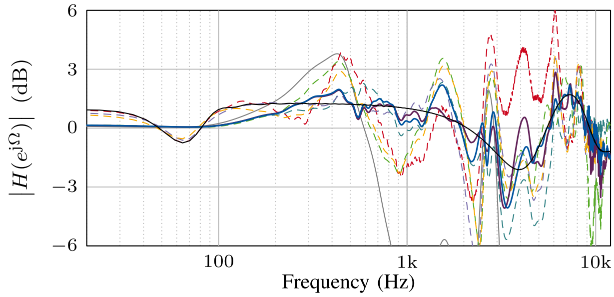

(b) Zoom into Fig. 5a.

FIGURE 5. **Magnitude response of aided transfer path for one person wearing balanced armature headphones.**

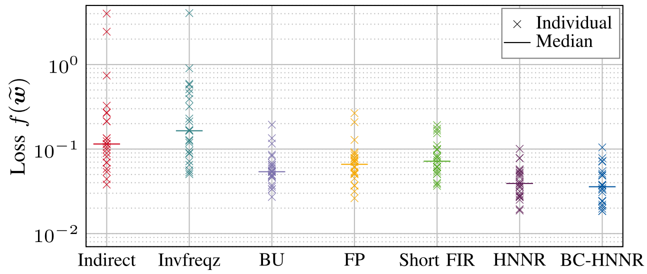

FIGURE 6. **Loss function values for 24 wearers using balanced armature headphones.**

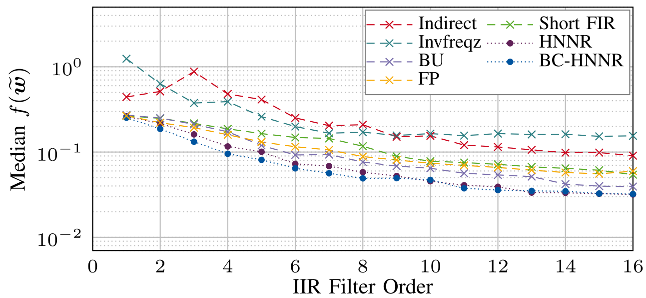

FIGURE 7. **Median of loss function values with 24 wearers using balanced armature headphones.**

proposed approaches decreases as N increases as restrictions due to small system orders become less significant.

D. BALANCED ARMATURE HEADPHONES HEAR-THROUGH

The analysis was repeated for the hearpiece database [66] which considers the transfer paths of 24 wearers of headphones that use balanced armature receivers. Fig. 5 shows the magnitude response of the aided transfer paths that result from the personalized hear-through filters. As before, the FIR filter uses $L_w = 512$ while the short FIR filter and all IIR filters use $N = 12$. The figure indicates the effect of the passive insulation for reference. With these headphones, the passive insulation mostly affects frequencies above 600 Hz.

The difference in results between the conventional algorithms is smaller compared to the dynamic driver headphones. Here, the indirect and invfreqz approaches yield the largest deviations from 0 dB, whereas the FP approach implements the target response more closely. The proposed HNNR and BC-HNNR algorithms reduce this deviation further. The corresponding loss function values are 0.115 for the conventional indirect method, 0.062, 0.055, 0.054, and 0.054 for the short FIR, invfreqz, BU, and FP methods, respectively, 0.027 for HNNR using $\mu = 6.9 \cdot 10^{-3}$ and 0.024 for BC-HNNR using $\mu = 2.6 \cdot 10^{-1}$. Here, the bias compensation allowed to increase μ as well, but with a smaller performance improvement.

Fig. 5(b) further illustrates the peaks of $|H(e^{j\Omega})|$, which assume maximum values of 6 dB at 6 kHz for the indirect approach, 3.55 dB at 1.55 kHz for the short FIR filter, 3.55 dB at 6.1 kHz for FP and BU, 2.84 dB at 6.1 kHz for HNNR, 2.23 dB at 1.54 kHz for invfreqz, and 2.17 dB at 7.3 kHz for BC-HNNR. The notch between 3 kHz and 6 kHz which invfreqz yields contributes to the comparatively high loss function value, but it should be noted that notches are generally less important than peaks with equivalent gain from a perceptual standpoint [69].

Fig. 6 shows the loss function values that the personalized 12-th order IIR filters achieve for the 24 wearers. It indicates that the short FIR filter performs well compared to other IIR-based approaches: the average and worst-case performance is superior to the indirect and invfreqz methods. This is in line with [10], which suggests to use short FIR filters in a similar application. Out of the conventional approaches, the FP method generally yields the lowest loss function values. The proposed HNNR and BC-HNNR algorithms yield an improvement by providing lower average-case and worst-case loss function values and a lower variation between wearers. Further, note that many DSPs feature programmable IIR filters. In these cases, the computational complexity of the short FIR filter is identical to the IIR filter, regardless of the fact that its IIR part may remain unused.

Fig. 7 shows the median of the loss function values across the 24 person-dependent filters for different IIR filter orders. In this experiment, invfreqz was the least reliable approach since its performance improved only slightly at higher orders. The best results with conventional methods were achieved by the BU approach at most filter orders. We observe that the bias compensation slightly improved upon these results,

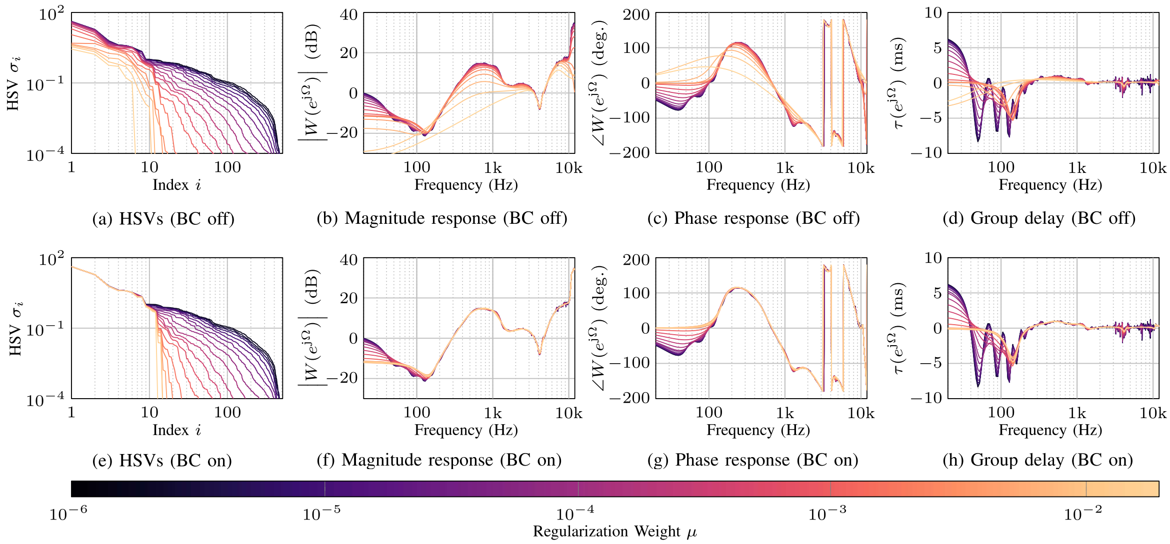

FIGURE 8. Effect of proposed regularization on the prototype hear-through filter for different regularization parameters μ. The top and bottom rows in the figure correspond to filters designed without and with bias compensation, respectively.

but the improvement turned out to be less significant for filter orders $N > 8$. IIR filters based on the proposed BC-HNNR with $N = 6$ perform roughly as well in terms of the MMSE loss function as those designed using the BU approach with $N = 10$, which corresponds to a reduction of the computational load by about 40 %. In contrast, a small but consistent improvement is obtained for equal filter orders.

E. EFFECT ON PROTOTYPE FIR FILTER

In this section, the effect of the proposed Hankel nuclear norm regularization on the prototype FIR filter is investigated. For brevity, one subject wearing dynamic driver headphones is considered. Fig. 8 shows the Hankel singular values and the magnitude and phase responses of the FIR filters that were designed for the same wearer that Fig. 2 corresponds to. The subfigures in the top and bottom rows correspond to filters which were obtained using the proposed HNNR and BC-HNNR algorithms, respectively. For clarity, only those filters which correspond to the 20 smallest values μ_m from the grid are shown. The BC-HNNR algorithm was configured to use an IIR filter order $N = 12$ for comparability with previous sections.

Fig. 8(a) shows that the penalty on $\|\mathcal{H}(\boldsymbol{w})\|_*$ reduced the magnitudes of all HSVs. Figs. 8(b) and 8(c) reveal that this caused a smoothing of the filter's magnitude and phase responses. Mostly, transfer function peaks and notches that cannot be implemented by low-order IIR filters were removed. Fig. 8(d) shows that the regularization also results in smaller peaks and notches in the group delay $\tau(e^{j\Omega})$. This is because the smoothing increases the phase response similarity of adjacent frequencies.

Although they belong to FIR filters, the transfer functions resembled those of an IIR filter more as μ increases. Large μ, however, changed the transfer function shape, which is mostly visible at the peaks of $|W(e^{j\Omega})|$ between 400 Hz and 1.2 kHz, and above 10 kHz. Note that these cases would yield large loss function values, which is why smaller μ values were used in the performance comparison.

Clearly, solving (15) introduced a bias of the first 12 HSVs towards zero, which is visible in the top figure. This is not intended because these HSVs do not contribute to the error bound (12). The figure reveals that the bias compensation greatly mitigated this effect. Compared to Fig. 8(a), Fig. 8(e) shows that the first $N = 12$ HSVs remained almost unaffected with BC-HNNR. This largely prevented the transfer function shape from changing as a result of the regularization, but reduced the IIR approximation error as intended. As a result, the bias-compensated Hankel nuclear norm regularization affected the transfer function shape less, which allowed using higher regularization parameters μ.

F. OPTIMAL REGULARIZATION PARAMETER

The previous sections determined the regularization parameter μ using a brute-force search, which required 32 executions of Algorithm 1 for each wearer. However, it would be beneficial to require fewer optimizations, especially for personalized filter designs. This section investigates the effect of the regularization parameter μ on the hear-through performance.

For the following analysis, let $\widetilde{\boldsymbol{w}}_m$ denote the impulse response of the filter that results from the proposed BC-HNNR algorithm with regularization parameter μ_m and subsequent approximation by a 12-th order IIR filter using BT. To quantify the effect of a suboptimally chosen regularization parameter, the loss function values of all 32 vectors $\widetilde{\boldsymbol{w}}_m$ are compared to the $\widetilde{\boldsymbol{w}}_m$ with index m that yields the lowest loss function value. This can be quantified using the relative loss deviation

$$f_{\text{rel.}}(\mu_m) = \frac{f(\widetilde{\boldsymbol{w}}_m)}{\min_{1\leq i\leq 32} f(\widetilde{\boldsymbol{w}}_i)} - 1. \tag{18}$$

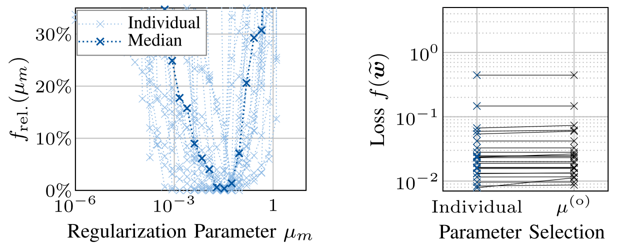

(a) Relative loss deviation caused by suboptimal choice of the parameter μ.

(b) Loss with individually-tuned versus constant μ.

FIGURE 9. **Effect of regularization parameter μ on hear-through performance for 23 wearers.**

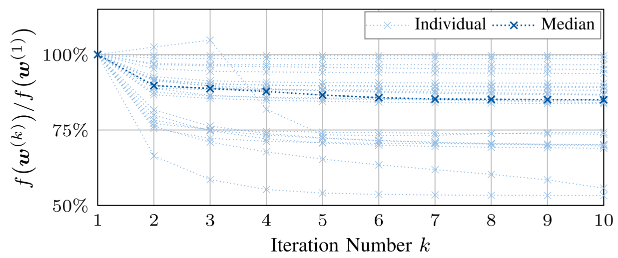

FIGURE 10. **Relative loss over iteration number k for 23 wearers.**

Fig. 9(a) depicts $f_{\mathrm{rel.}}(\mu_m)$ for 32 discrete values μ_m and all 23 wearers, as well as the median across wearers for each μ_m. For clarity, the figure excludes values above 35%. It indicates a dependence of the optimal μ on the wearer. For all wearers, the optimal parameter μ which yielded $f_{\mathrm{rel.}}(\mu_m) = 0$ was in the range $10^{-3} < \mu < 1$.

The observed similarity in parameter choices across wearers and the amount of overlap in $f_{\mathrm{rel.}}(\mu_m)$ motivates us to define an order- and headphone-specific optimal regularization parameter $\mu^{(\mathrm{o})}$. For optimal median performance using a single, a-priori selected regularization parameter, one can fix μ to $\mu^{(\mathrm{o})}$, which we define as the regularization parameter that minimizes the median loss across 23 wearers. This lead to $\mu^{(\mathrm{o})} = 3.28 \cdot 10^{-2}$ in the present case. If μ is fixed in this way, the number of executions of Algorithm 1 reduces from 32 to just one.

Although fixing $\mu = \mu^{(\mathrm{o})}$ yielded optimal performance for some wearers, it lead to inferior performance for others compared to the brute-force search because the optimal parameter μ is generally wearer-dependent. Fig. 9(b) indicates the effect of fixing $\mu = \mu^{(\mathrm{o})} = 3.28 \cdot 10^{-2}$ on the loss for all wearers. The marks on the left are the same as those in Fig. 3, whereas marks on the right correspond to the single-shot optimization using $\mu^{(\mathrm{o})}$. Identical wearers are indicated by lines between marks for clarity. The figure shows that both algorithms yielded virtually the same loss for 21 of the 23 wearers, with a minor performance degradation for the other 2 wearers.

In summary, the analysis suggests that the value range of μ can be narrowed significantly with negligible performance degradation. In applications where minor performance setbacks are acceptable, μ can be set to a fixed value based on a-priori knowledge. The performance appears to be insensitive towards the parameter choice if μ remains within the aforementioned value range.

G. NUMBER OF BIAS COMPENSATION ITERATIONS

To provide users with immediate feedback of the equalization performance, a quick termination of the algorithm within a fixed and low number of iterations is crucial. This section examines the number of bias compensation iterations K that is required in practice. The calibration of a 12-th-order IIR filter to the 23 wearers of dynamic driver headphones is considered as one example. The regularization parameter μ was chosen optimally as previously described.

To quantify the improvement of the iterative BC-HNNR algorithm, the loss $f(\boldsymbol{w}^{(k)})$ at successive iterations is related to the loss obtained from using the initial iterate $f(\boldsymbol{w}^{(1)})$. Fig. 10 depicts the resulting relative loss associated with the filter optimization for 23 individual wearers, as well as the median progression. These percentages indicate the loss reduction compared to the initial estimate.

Generally, the obtained improvement depended on the wearer. It amounted to a minimum of 5% and a maximum of around 40%. The median progression reveals that most of the improvement was obtained from the first iterations. Further improvements were achieved up to the 6-th iteration, but diminished rapidly thereafter. This trend was reflected in the majority of the wearers, which suggests that few iterations are sufficient to improve the initial estimate of the strong subspace to sufficient accuracy. With 5 of the 23 wearers, the improvement became negligible after only 2 iterations. It is also evident that more iterations do not always improve performance, as is the case for the one wearer which increased the loss in the first three iterations. Nevertheless, the bias compensation yielded an improvement after the third iteration in all cases.

The analysis suggests two ways to reduce number of iterations K which ease the computational load of the proposed BC-HNNR algorithm. In the considered setting, $K < 10$ was sufficient to guarantee algorithm convergence for all wearers. As a further improvement, an adaptive stopping criterion which terminates the algorithm once successive iterations no longer improve the performance could be adopted.

VI. CONCLUSION

We propose an indirect IIR filter design algorithm for the personalization of the listening impression when wearing headphones, hearables, or hearing aids. Using the nuclear norm heuristic, the algorithm mitigates the performance degradation of indirect algorithms that the post-hoc IIR approximation of the prototype FIR filter causes. The bias which the nuclear norm heuristic introduces is investigated, and a compensation mechanism is adopted. The resulting approximation-aware time-domain filter synthesis retains the advantages of conventional indirect algorithms such as guaranteed convergence and stability, but uses a targeted penalization of the IIR approximation error using a compensation mechanism in the prototype filter design stage to obtain reliable results.

We evaluated the performance of the proposed algorithm empirically, using the personalization of a hear-through filter as one example. Therefore, real-world measurement data obtained from multiple wearers and two headphones was used. The effect of the regularizer on the designed filter is illustrated, and it is shown how algorithm parameters such as the weight of the regularization and the number of bias compensation iterations can be favorably selected. The proposed algorithm shows high robustness against transfer path variations and consistently higher performance than conventional indirect and direct algorithms at equal system orders. The high robustness and interpretability of the results suggest that the presented algorithm is well-suited for the personalization of hearing devices in practical applications.

REFERENCES

[1] B. Edwards, "Understanding new and emerging categories of hearing devices," *ENT Audiol. News*, vol. 28, no. 5, pp. 51–52, Dec. 2019.
[2] R. Gupta et al., "Augmented/mixed reality audio for hearables: Sensing, control, and rendering," *IEEE Signal Process. Mag.*, vol. 39, no. 3, pp. 63–89, May 2022.
[3] H. Y. Seol and I. J. Moon, "Hearables as a gateway to hearing health care," *Clin. Exp. Otorhinolaryngol.*, vol. 15, no. 2, pp. 127–134, Mar. 2022.
[4] M. Hiipakka, M. Tikander, and M. Karjalainen, "Modeling the external ear acoustics for insert headphone usage," *J. Audio Eng. Soc.*, vol. 58, pp. 269–281, May 2010.
[5] F. Denk, S. D. Ewert, and B. Kollmeier, "On the limitations of sound localization with hearing devices," *J. Acoust. Soc. America*, vol. 146, no. 3, pp. 1732–1744, Sep. 2019.
[6] H. Schepker, F. Denk, B. Kollmeier, and S. Doclo, "Acoustic transparency in hearables—Perceptual sound quality evaluations," *J. Audio Eng. Soc.*, vol. 68, no. 7/8, pp. 495–507, Jul. 2020.
[7] J. Rämö and V. Välimäki, "Digital augmented reality audio headset," *J. Electr. Comput. Eng*, vol. 2012, no. 1, Oct. 2012, Art. no. 457374.
[8] V. Välimäki, A. Franck, J. Rämö, H. Gamper, and L. Savioja, "Assisted listening using a headset: Enhancing audio perception in real, augmented, and virtual environments," *IEEE Signal Process. Mag.*, vol. 32, no. 2, pp. 92–99, Mar. 2015.
[9] J. Rämö and V. Välimäki, "An allpass hear-through headset," in *Proc. Eur. Signal Process. Conf.*, Lisbon, Portugal, Sep. 2014, pp. 1123–1127.
[10] F. Denk, H. Schepker, S. Doclo, and B. Kollmeier, "Equalization filter design for achieving acoustic transparency in a semi-open fit hearing device," in *Proc. ITG Conf. Speech Commun.*, Oldenburg, Germany, Oct. 2018, pp. 1–5.
[11] J. Fabry, F. König, S. Liebich, and P. Jax, "Acoustic equalization for headphones using a fixed feed-forward filter," in *Proc. IEEE Int. Conf. Acoust. Speech Signal Process.*, Brighton, U.K., May 2019, pp. 980–984.
[12] F. Denk, H. Schepker, S. Doclo, and B. Kollmeier, "Acoustic transparency in hearables—Technical evaluation," *J. Audio Eng. Soc.*, vol. 68, no. 7/8, pp. 508–521, Jul. 2020.
[13] A. T. Sabin, D. J. Van Tasell, B. Rabinowitz, and S. Dhar, "Validation of a self-fitting method for over-the-counter hearing aids," *Trends Hear.*, vol. 24, Jan. 2020, Art. no. 2331216519900589.
[14] R. Gupta, R. Ranjan, J. He, W.-S. Gan, and S. Peksi, "Acoustic transparency in hearables for augmented reality audio: Hear-through techniques review and challenges," in *Proc. Int. Conf. Audio Virtual Augmented Reality*, Redmond, WA, USA, Aug. 2020, pp. 110–119.
[15] J. Fabry and P. Jax, "Primary path estimator based on individual secondary path for ANC headphones," in *Proc. IEEE Int. Conf. Acoust. Speech Signal Process.*, Barcelona, Spain, May 2020, pp. 456–460.
[16] W. Jin, T. Schoof, and H. Schepker, "Individualized hear-through for acoustic transparency using PCA-based sound pressure estimation at the eardrum," in *Proc. IEEE Int. Conf. Acoust. Speech Signal Process.*, Singapore, May 2022, pp. 341–345.
[17] K. Fink and L. Ray, "Tuning principal component weights to individualize HRTFs," in *Proc. IEEE Int. Conf. Acoust. Speech Signal Process.*, Kyoto, Japan, Mar. 2012, pp. 389–392.
[18] V. Jayaram, I. Kemelmacher-Shlizerman, and S. M. Seitz, "HRTF estimation in the wild," in *Proc. Annu. ACM Symp. User Interface Softw.* Technol, San Francisco, CA, USA, Oct. 2023, pp. 1–9.
[19] D. Fantini, M. Geronazzo, F. Avanzini, and S. Ntalampiras, "A survey on machine learning techniques for head-related transfer function individualization," *IEEE Open J. Signal Process.*, vol. 6, pp. 30–56, 2025.
[20] R. Ranjan and W.-S. Gan, "Natural listening over headphones in augmented reality using adaptive filtering techniques," *IEEE/ACM Trans. Audio Speech Lang. Process.*, vol. 23, no. 11, pp. 1988–2002, Nov. 2015.
[21] J. Liski, R. Väänänen, S. Vesa, and V. Välimäki, "Adaptive equalization of acoustic transparency in an augmented-reality headset," in *Proc. Audio Eng. Soc. Int. Conf. Headphone Technol.*, Aalborg, Denmark, Aug. 2016, no. 6–4, pp. 169–176.
[22] R. Gupta, M. Karthik, and Y. Palanivel, "Low complex IIR adaptive hear-through ambient filtering for overcoming practical constraints in earbuds," in *Proc. Interspeech*, Rotterdam, The Netherlands, Aug. 2025, pp. 3115–3119.
[23] V. Patel, J. Cheer, and S. Fontana, "Design and implementation of an active noise control headphone with directional hear-through capability," *IEEE Trans. Consum. Electron.*, vol. 66, no. 1, pp. 32–40, Feb. 2020.
[24] C.-R. Huang, C.-Y. Chang, and S. M. Kuo, "Time-Shift modeling-based hear-through system for in-ear headphones," *IEEE Trans. Consum. Electron.*, vol. 68, no. 3, pp. 273–280, Aug. 2022.
[25] H. Watanabe and T. Terada, "Transparency mode of hearable reduces your spatial hearing: Evaluation and cancelling method to restore spatial hearing," *IEEE Access*, vol. 11, pp. 97952–97960, 2023.
[26] H. Schepker, F. Denk, B. Kollmeier, and S. Doclo, "Robust single- and multi-loudspeaker least-squares-based equalization for hearing devices," *EURASIP J. Audio Speech Music Process.*, vol. 2022, no. 1, Jun. 2022, Art. no. 15.
[27] L. Litwin, "FIR and IIR digital filters," *IEEE Potentials*, vol. 19, no. 4, pp. 28–31, Oct./Nov. 2000.
[28] F. Hilgemann, J. Fabry, and P. Jax, "Design of IIR filters for active noise control by constrained optimization," in *Proc. Eur. Signal Process. Conf.*, Dublin, Ireland, Aug. 2021, pp. 151–155.
[29] G. Ramos and J. J. López, "Filter design method for loudspeaker equalization based on IIR parametric filters," *J. Audio Eng. Soc.*, vol. 54, pp. 1162–1178, Dec. 2006.
[30] P. Dodds, "A flexible numerical optimization approach to the design of biquad filter cascades," in *Proc. Audio Eng. Soc. Int. Conv.*, New York, NY, USA, Oct. 2020, pp. 1–9.
[31] A. Betser and E. Zeheb, "Reduced order IIR approximation to FIR digital filters," *IEEE Trans. Signal Process.*, vol. 39, no. 11, pp. 2540–2544, Nov. 1991.
[32] A. Jiang and H. K. Kwan, "IIR digital filter design with new stability constraint based on argument principle," *IEEE Trans. Circuits Syst. I, Reg. Papers*, vol. 56, no. 3, pp. 583–593, Mar. 2008.
[33] Y. Zhuang and Y. Liu, "A stable IIR filter design approach for high-order active noise control applications," *Acoustics*, vol. 5, no. 3, pp. 746–758, Jul. 2023.
[34] F. Hilgemann, C. Weyer, and P. Jax, "Design of low-order IIR filters based on Hankel nuclear norm regularization for achieving acoustic transparency," in *Proc. ITG Conf. Speech Commun.*, Aachen, Germany, Sep. 2023, pp. 136–140.
[35] F. Hilgemann and P. Jax, "Low-Order controllers for active noise cancellation based on Hankel matrix rank minimization," in *Proc. Int. Workshop Acoust. Sig. Enhancement*, Aalborg, Denmark, Sep. 2024, pp. 399–403.
[36] E. J. Candès and T. Tao, "The power of convex relaxation: Near-optimal matrix completion," *IEEE Trans. Inf. Theory*, vol. 56, no. 5, pp. 2053–2080, May 2010.
[37] K. Usevich and P. Comon, "Hankel low-rank matrix completion: Performance of the nuclear norm relaxation," *IEEE J. Sel. Topics Signal Process.*, vol. 10, no. 4, pp. 637–646, Jun. 2016.

[38] M. Fazel, H. Hindi, and S. Boyd, "A rank minimization heuristic with application to minimum order system approximation," in *Proc. America Control Conf.*, Arlington, VA, USA, Jun. 2001, vol. 6, pp. 4734–4739.
[39] M. Fazel, T. K. Pong, D. Sun, and P. Tseng, "Hankel matrix rank minimization with applications to system identification and realization," *SIAM J. Matrix Anal. Appl.*, vol. 34, no. 3, pp. 946–977, Jul. 2013.
[40] N. Yair and T. Michaeli, "Multi-Scale weighted nuclear norm image restoration," in *Proc. IEEE Conf. Comput. Vis. Pattern Recognit.*, Salt Lake City, UT, USA, Jun. 2018, pp. 3165–3174.
[41] Y. Hu, D. Zhang, J. Ye, X. Li, and X. He, "Fast and accurate matrix completion via truncated nuclear norm regularization," *IEEE Trans. Pattern Anal. Mach. Intell.*, vol. 35, no. 9, pp. 2117–2130, Sep. 2013.
[42] S. Gu, L. Zhang, W. Zuo, and X. Feng, "Weighted nuclear norm minimization with application to image denoising," in *Proc. IEEE Conf. Comput. Vis. Pattern Recognit.*, Columbus, OH, USA, Jun. 2014, pp. 2862–2869.
[43] F. Wen, L. Chu, P. Liu, and R. C. Qiu, "A survey on nonconvex regularization-based sparse and low-rank recovery in signal processing, statistics, and machine learning," *IEEE Access*, vol. 6, pp. 69883–69906, 2018.
[44] Z. Hu, F. Nie, R. Wang, and X. Li, "Low rank regularization: A review," *Neural Netw.*, vol. 136, pp. 218–232, Apr. 2021.
[45] Z. Luo, D. Shi, J. Ji, X. Shen, and W.-S. Gan, "Real-time implementation and explainable AI analysis of delayless CNN-based selective fixed-filter active noise control," *Mech. Syst. Signal Process.*, vol. 214, May 2024, Art. no. 111364.
[46] O. Kirkeby and P. A. Nelson, "Digital filter design for inversion problems in sound reproduction," *J. Audio Eng. Soc.*, vol. 47, no. 7/8, pp. 583–595, Jul. 1999.
[47] T. Xiao and S. Doclo, "Effect of target signals and delays on spatially selective active noise control for open-fitting hearables," in *Proc. IEEE Int. Conf. Acoust. Speech Signal Process.*, Seoul, Korea, 2024, pp. 1056–1060.
[48] C. Burrus and T. Parks, "Time domain design of recursive digital filters," *IEEE Trans. Audio Electroacoust.*, vol. 18, no. 2, pp. 137–141, Jun. 1970.
[49] K. Steiglitz and L. McBride, "A technique for the identification of linear systems," *IEEE Trans. Autom. Control*, vol. 10, no. 4, pp. 461–464, Oct. 1965.
[50] J. E. Dennis Jr and R. B. Schnabel, *Numerical Methods for Unconstrained Optimization and Nonlinear Equations*. Englewood Cliffs, NJ: SIAM, 1996.
[51] H. Brandenstein and R. Unbehauen, "Least-squares approximation of FIR by IIR digital filters," *IEEE Trans. Signal Process.*, vol. 46, no. 1, pp. 21–30, Jan. 1998.
[52] H. Brandenstein and R. Unbehauen, "Weighted least-squares approximation of FIR by IIR digital filters," *IEEE Trans. Signal Process.*, vol. 49, no. 3, pp. 558–568, Mar. 2001.
[53] B. Moore, "Principal component analysis in linear systems: Controllability, observability, and model reduction," *IEEE Trans. Autom. Control*, vol. 26, no. 1, pp. 17–32, Feb. 1981.
[54] L. Pernebo and L. Silverman, "Model reduction via balanced state space representations," *IEEE Trans. Autom. Control*, vol. 27, no. 2, pp. 382–387, Apr. 1982.
[55] B. Beliczynski, I. Kale, and G. D. Cain, "Approximation of FIR by IIR digital filters: An algorithm based on balanced model reduction," *IEEE Trans. Signal Process.*, vol. 40, no. 3, pp. 532–542, Mar. 1992.
[56] S. Gugercin and A. C. Antoulas, "A survey of model reduction by balanced truncation and some new results," *Int. J. Control*, vol. 77, no. 8, pp. 748–766, Apr. 2004.
[57] A. Walker, "Large-sample estimation of parameters for autoregressive processes with moving-average residuals," *Biometrika*, vol. 49, no. 1/2, pp. 117–131, 1962.
[58] S. Boyd and L. Vandenberghe, *Convex Optimization*. Cambridge, U.K.: Cambridge Univ. Press, 2004.
[59] B. Recht, M. Fazel, and P. A. Parrilo, "Guaranteed minimum-rank solutions of linear matrix equations via nuclear norm minimization," *SIAM Rev.*, vol. 52, no. 3, pp. 471–501, Jan. 2010.
[60] M. Frank and P. Wolfe, "An algorithm for quadratic programming," *Nav. Res. Logistics Quart.*, vol. 3, no. 1/2, pp. 95–110, 1956.
[61] Z. Liu and L. Vandenberghe, "Interior-point method for nuclear norm approximation with application to system identification," *SIAM J. Matrix Anal. Appl.*, vol. 31, no. 3, pp. 1235–1256, Apr. 2010.
[62] S. Boyd, N. Parikh, E. Chu, B. Peleato, and J. Eckstein, "Distributed optimization and statistical learning via the alternating direction method of multipliers," *Found. Trends Mach. Learn.*, vol. 3, no. 1, pp. 1–122, 2011.
[63] Z. Liu, A. Hansson, and L. Vandenberghe, "Nuclear norm system identification with missing inputs and outputs," *Syst. Control Lett.*, vol. 62, no. 8, pp. 605–612, Aug. 2013.
[64] M. A. Stone, B. C. Moore, K. Meisenbacher, and R. P. Derleth, "Tolerable hearing aid delays. V. Estimation of limits for open canal fittings," *Ear Hear.*, vol. 29, no. 4, pp. 601–617, Aug. 2008.
[65] S. Liebich, J. Fabry, P. Jax, and P. Vary, "Acoustic path database for ANC in-ear headphone development," in *Proc. Int. Congr. Acoust.*, Aachen, Germany, Sep. 2019, pp. 4326–4333.
[66] F. Denk and B. Kollmeier, "The hearpiece database of individual transfer functions of an in-the-ear earpiece for hearing device research," *Acta Acust.*, vol. 5, no. 2, pp. 1–16, Jan. 2021.
[67] B. Bank, "Multichannel equalization and crosstalk cancellation using fixed-pole IIR filters," *J. Audio Eng. Soc.*, vol. 66, pp. 901–909, Nov. 2018.
[68] B. Bank, "Warped, Kautz, and fixed-pole parallel filters: A review," *J. Audio Eng. Soc.*, vol. 70, no. 6, pp. 414–434, Jun. 2022.
[69] R. Bücklein, "The audibility of frequency response irregularities," *J. Audio Eng. Soc.*, vol. 29, no. 3, pp. 126–131, Mar. 1981.